

Design of Experiments: application to the reliability assessment of MEMS devices - (Revision 2)

Matteo Macchini¹, Maxime Auchlin¹, Alessio Mancinelli¹, and Ivan Marozau²

¹EPFL

²CSEM (advisor)

March 1, 2018

Abstract

This report presents the application of the Plackett-Burman design of experiment to a reliability study of a 3-axis commercial accelerometer based on MEMS (MicroElectro-Mechanical System). The aim is to observe the lifetime of the devices undergoing shock testing at 4,500g, after having been through different environmental conditions supposed to be representative of the space environment. In the study, 7 different parameters are analyzed: the first step is environmental, with temperature and humidity being varied. The second step consists in the application of a mechanical solicitation, in the form of a vibration test with varying frequencies and peak accelerations. The considered response is the number of cycles of a sequence of shocks along all axes of the device, necessary to produce total failure. The experimental results are used in order to compute the relative half-effects and evaluate the corresponding normal plots for the error analysis.

Introduction

Nowadays reliability qualification tests for space applications are based on MIL, NASA or ESA standards, the purpose being to ensure that a device will perform nominally for a specified lifetime. Those tests can help to understand which are the root-causes of the failure, in order to mitigate them. However almost every testing procedure relies on the survival rate while considering a single external constraint.

It is useful to point out, in a first discussion, that in their standard form they might fail to accurately represent real operation conditions, where loads of different nature can simultaneously stress the device. For example, the storage and then preparation on the launch pad in French Guiana (the European spaceport) consists in a heterogeneous set of tests, from a sequence of temperature and humidity oscillations, to intense vibrations and shock in order to simulate the launch and the separations of the different rocket's stages .

This work therefore provides a first view of the 8-runs 7-factors application of the Plackett-Burman design. Two models are considered to represent the experience: the first takes into account the main effects and the second takes into account the interactions. The aim is to observe any possible effect of the succession of thermal and mechanical stress tests. A matrix of alias is computed in order to reveal any hidden interactions. Finally, a selection of effects and secondary interactions is performed as well as an evaluation of their possible random behavior. Figure 1 depicts the strategy used:

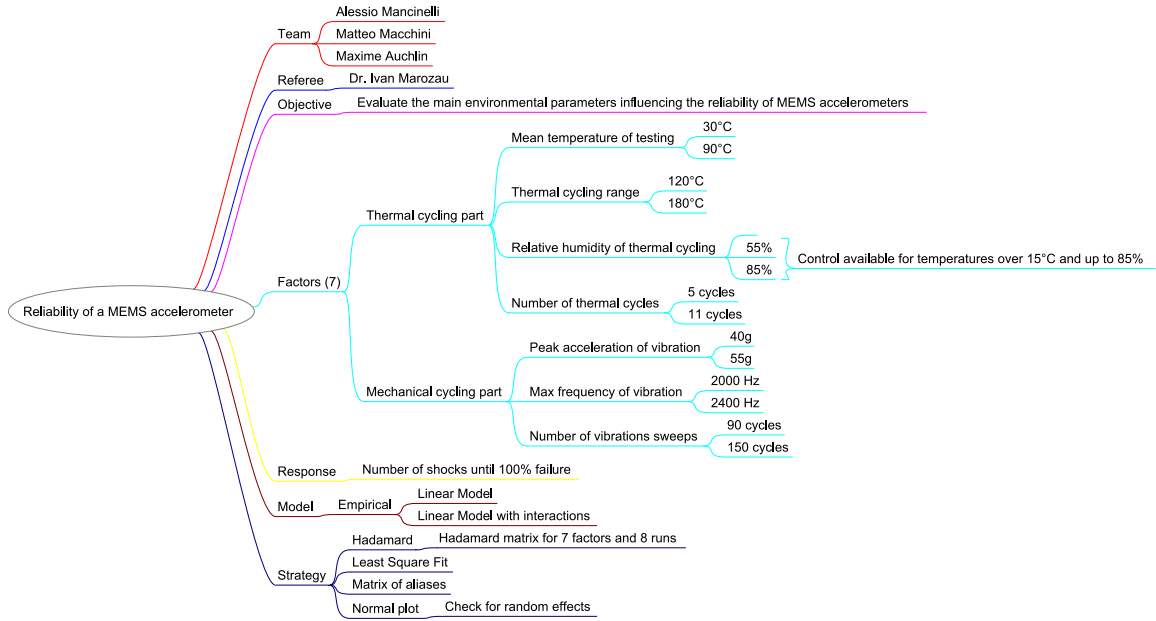


Figure 1: Mind map of the strategy.

Experimental part

Choice of experience and design

The testing method is based on a previous study – named MEMS-REAL – from CSEM on the reliability assessment of MEMS-based components for space applications. A new method was developed, based on ESA and US military standards, for components that are to be dedicated for space applications. The method from MEMS-REAL is explained in the following paragraph.

Initially, a restricted set of five samples are tested over cycles with increasing load (*i.e.* 20% greater temperature range, vibrations intensity, etc.) starting from the manufacturer’s nominal range of operation, until complete failure occurs. This first step is necessary to define the limit to which the devices can be pushed to. The load can be provided by thermal cycling, thermal shocks, mechanical cycling (*i.e.* vibrations), mechanical shocks or pressure cycling. These stress tests are chosen in order to represent, as well as possible, the conditions that the device will undergo during spaceborne operations. The second step consists in the application of a load that represents 25% of the maximum value obtained from the first test. This time, 20 samples are necessary and one evaluates of the number of cycles necessary to reach 100% of failure of the devices under a given unique load. A Weibull statistics is then drawn and the characteristic lifetime of the chosen device is defined.

MEMS-REAL’s method features three drawbacks:

- a great number of samples is needed for each company willing to evaluate and then qualify a product for space,
- performing of time consuming experiments on this large number of samples,

- no consideration of possible interactions.

These points can supposedly be mitigated by a good design, hence the choice of a Plackett-Burman design as exploratory test plan. This report therefore aims at verifying the applicability of the design of experiments to MEMS reliability assessment.

Test vehicle

Japanese manufacturer Murata is producing the SCA-3100 with capabilities summarized in Figure 2:



| | | | |
|---|---------|---|----------------|
|  | |  | |
| Size: 7.60 x 3.30 x 8.60 mm | | Model: SCA3100-D04 | |
| | | Description: 3-axis high performance accelerometer with digital PSI interface | |
| MEMS type: | | 3-axis linear accelerometer | |
| Dedicated software: | | No | |
| Computer interface: | | SPI interface | |
| Compatibility with mechanical testing: | | Yes | |
| Compatibility w/ environmental testing: | | Not fully (FR4 eval. board) | |
| Maturity: | High | Acceleration range: | ±2g |
| Package: | Polymer | Temperature range: | -40°C to 125°C |

Figure 2: Murata's 3-axis MEMS accelerometer's characteristics.

The polymeric package is filled with a gel, designed to damp excessive vibration and shocks, hence protecting the silicon subsystems and metallic wire-bondings from fracture. This feature made the sample particularly tough to brake during the vibration test campaign run in MEMS-REAL. A property also found in the present study, even with the devices having been through a first step of thermal testing.

Equipment

The experimental part has been done at CSEM in Neuchâtel, in the *Advanced Manufacturing and Components Reliability* group. The focus has been given to environmental testing (namely thermal cycling and humidity ingress combined), vibrations testing and mechanical shocks.

The environmental chamber ESPEC SH-662 permits to cycles between -60°C to +180°C at maximum ramp-up rates of 2.5°C/min and ramp-down 1.7°C/min . Humidity can be controlled over the range 15°C to 85°C for 85%RH. Outside of these bounds the humidity cannot be controlled.

For the vibrations testing, a low-force shaker for payloads up to 25kg is used. The Brüel & Kjær LDS V555 enables vibrations of frequencies up to 2400 Hz and accelerations up to 100g when empty. With the test jig and sample attached, the maximum load achievable is limited to 55g. A reference accelerometer is screwed on the test jig, enabling active control of the frequency and the acceleration.

Finally, the response of the experiment is set to be the number of mechanical shocks at 4,500g necessary to lead to a complete failure of the sensor. The shock testing machine, a Shinyei PST-300, is made of a pendulum, on the backplate of which the sample is fixed . The pendulum can be lifted at a certain angle

and then released, leading it to fall and come hit a bumper placed at 0°, with a given kinetic energy. The bumper can be chosen of different materials in order to cover a range of 5 to 10,000g, with a 2% variation over reproducibility and a reference accelerometer acquires the magnitude of the shocks for control.

Test plan

A Hadamard matrix for 2^3 runs is obtained from Matlab by using the appropriate function `X=hadamard(8)`. The names of the corresponding samples are indicated next to each line:

$$X = \begin{pmatrix} 1 & 1 & 1 & 1 & 1 & 1 & 1 & 1 \\ 1 & -1 & 1 & -1 & 1 & -1 & 1 & -1 \\ 1 & 1 & -1 & -1 & 1 & 1 & -1 & -1 \\ 1 & -1 & -1 & 1 & 1 & -1 & -1 & 1 \\ 1 & 1 & 1 & 1 & -1 & -1 & -1 & -1 \\ 1 & -1 & 1 & -1 & -1 & 1 & -1 & 1 \\ 1 & 1 & -1 & -1 & -1 & -1 & 1 & 1 \\ 1 & -1 & -1 & 1 & -1 & 1 & 1 & -1 \end{pmatrix} \begin{matrix} \text{T08} \\ \text{T06} \\ \text{T02} \\ \text{T10} \\ \text{T07} \\ \text{T05} \\ \text{T01} \\ \text{T09} \end{matrix} \quad (1)$$

The factors are summarised hereafter:

| | | | | | |
|---|---|---------------------------------|------|------|------|
| 1 | A | Mean temperature | [°C] | 30 | 90 |
| 2 | B | Range of cycling | [°C] | 120 | 180 |
| 3 | C | Dryness [1-(Relative humidity)] | [%] | 15 | atm |
| 4 | D | Number of thermal cycles | [-] | 5 | 10 |
| 5 | E | Peak acceleration of vibration | [g] | 40 | 55 |
| 6 | F | Maximum frequency of vibration | [Hz] | 2000 | 2400 |
| 7 | G | Vibration cycling | [-] | 90 | 150 |

Figure 3: Experimental factors tested following the Hadamard matrix. Due to swapped humidity conditions, factor C (humidity initially) has been redefined as the level of dryness, being equivalent to 1-(Relative Humidity). “atm” defines ambient (atmospheric) humidity of the laboratory.

The experimental procedure is separated over 3 phases: the thermal-environmental phase with the combination of factors A, B, C and D. Following is the mechanical step with factors E, F and G over the three axes of the device (X-Y-Z sequentially). Finally, the samples are fixed on the back-plate of the pendulum of the shocks machine and undergo series of 6x5 shocks in all of the 6 main directions of the device. After this sequence, the sample is removed from the jig and its capability to measure the value of gravity is checked. A device is considered as failed either when gravity cannot be measured accurately, either if complete failure occurs.

First step: Thermal-environmental testing

Normally, thermal cycling procedure is either dictated by a standard (MIL-STD-883K, Method 2002), either limited by the apparatus. In the case of this study, the limits of the environmental chamber (ESPEC SH-662) are taken as lower and upper bound. As for the temporal conditions of the thermal cycling procedure, it was proposed to deviate from the standard conditions significantly. Figure 4 shows the thermal cycles built from the matrix of test. The factors has been set on the legacy obtained from MEMS-REAL in order not to overstress the samples in this first step.

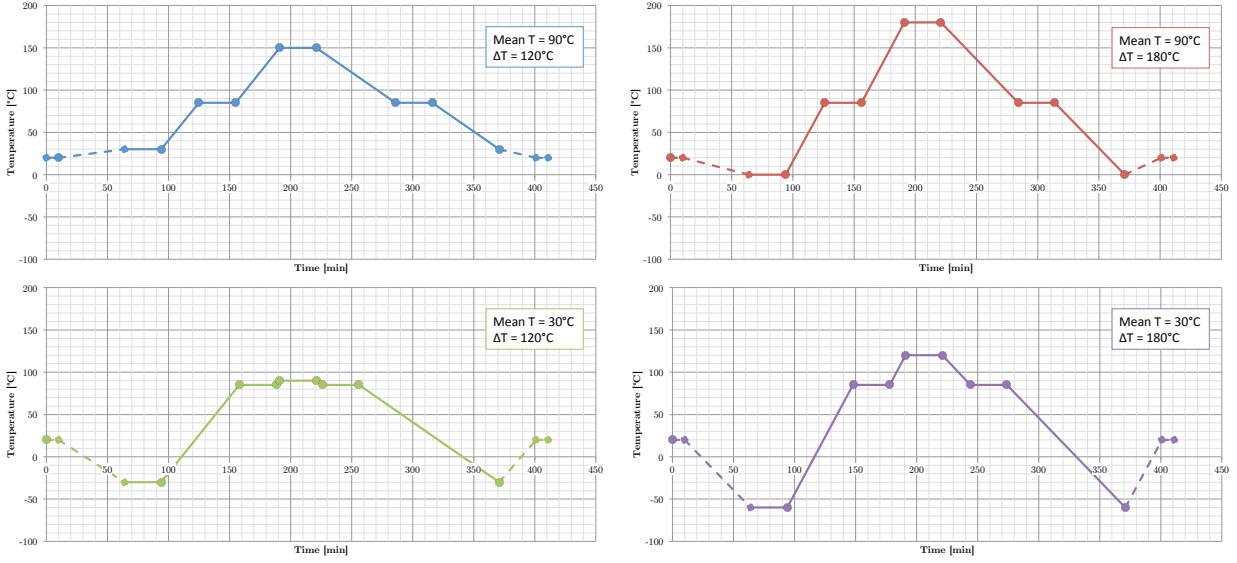


Figure 4: Depiction of the thermal cycles following the factors defined in Figure 3 and the test matrix X. A cycle consists in the solid line curves, while the dashed part indicate the initial and end sequences.

Special care has been taken to guarantee the same soak time in the chamber, meaning that different heating and cooling duration have been adapted for each run since the mean temperatures and ranges vary. As a consequence, the time spent in the chamber for a single cycle is rigorously the same for any condition: 5 hours and 7 minutes. Starting conditions are also set accordingly, so that the time needed to reach the first set point, from ambient conditions, remains constant. It is to be noted that if the sample has to be removed from the chamber before the end of the maximum number of cycles, the chamber is opened only when the inside temperature matches the ambient, in order not to open it when the inside temperature is smaller than the ambient (risk of condensation and icing).

Second step: Vibration testing

The starting frequency is set at 5 Hz and increases at a rate of 2 octaves per minute until reaching the set point. This test is inspired from MIL-STD-883J (Method 2005.2). The software automatically tunes the increase of g , since the physical limitation of the apparatus does not allow displacements big enough to reach the acceleration set point at low frequencies.

The definition of a sweep is a logarithmical round trip from 5 Hz to either 2,000 or 2,400 Hz – and back again to 5 Hz following the same path. The duration of a single sweep is 8 minutes and 30 seconds. It is important to point out that vibration testing in the MEMS-REAL study never managed to show any failure in the accelerometers produced by Murata. During the present study, no failure after vibrations testing was also recorded.

Third step: Mechanical shocks (response)

The first and second steps have been scaled so that 100% of the samples survived until this third step. The number of shocks necessary to reach total failure were known from the previous MEMS-REAL tests and

used as comparison (Figure 5).

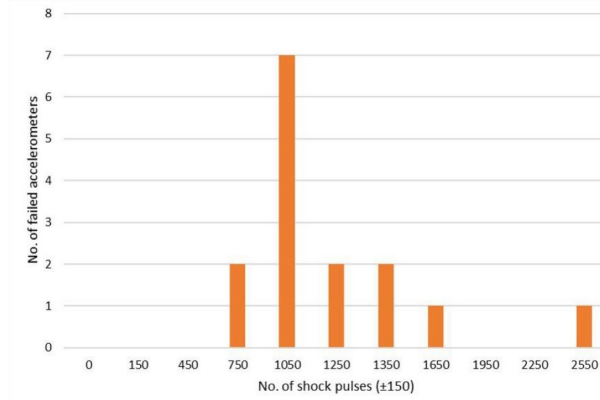


Figure 5: Histogram of the number of failed Murata devices from MEMS-REAL. In this case, shock testing was applied on pristine samples. [1]

Once the sample is observed to give inconsistent values of the acceleration (g-value) or no signal at all, it is considered as broken. Another round of shocks (6x5 in all main directions) is then done in order to confirm the non-reversibility of the failure, meaning that some element in the component is physically out-of-order.

Results and analysis

The following table shows the experimental conditions and the response:

| Code> | A | B | | | C | | D | E | F | G | Y |
|-------|--------|-------|--------|--------|-----|-----|--------|--------|---------|--------|----------|
| Run | Mean T | Range | (Tmax) | (Tmin) | RH | | Cycles | Peak g | FreqMax | Cycles | Response |
| T08 | 1 | 90 | 180 | 180 | 0 | atm | 10 | 55 | 2400 | 150 | 30 |
| T06 | 2 | 30 | 180 | 120 | -60 | 85 | 10 | 40 | 2400 | 90 | 30 |
| T02 | 3 | 90 | 120 | 150 | 30 | 85 | 10 | 55 | 2000 | 90 | 150 |
| T10 | 4 | 30 | 120 | 90 | -30 | atm | 10 | 40 | 2000 | 150 | 790 |
| T07 | 5 | 90 | 180 | 180 | 0 | atm | 5 | 40 | 2000 | 90 | 150 |
| T05 | 6 | 30 | 180 | 120 | -60 | 85 | 5 | 55 | 2000 | 150 | 90 |
| T01 | 7 | 90 | 120 | 150 | 30 | 85 | 5 | 40 | 2400 | 150 | 280 |
| T09 | 8 | 30 | 120 | 90 | -30 | atm | 5 | 55 | 2400 | 90 | 60 |

Linear model

Since the test plan has been built following a Hadamard matrix, the resulting orthogonal matrix comes in handy when dealing with the computation of the matrix of dispersion, which translate into for the Least Square Fit algorithm:

$$\hat{a} = (X^T X)^{-1} X^T Y \equiv \frac{1}{N} I_N X^T Y \quad (2)$$

With $N=8$, X being given in Equation 1 and Y from Table 2. Computing this equation gives the half-effects and their relative half-effects of the 7 factors:

$$\begin{pmatrix} \alpha_0 \\ \alpha_1 \\ \alpha_2 \\ \alpha_3 \\ \alpha_4 \\ \alpha_5 \\ \alpha_6 \\ \alpha_7 \end{pmatrix} = \begin{pmatrix} 197.5 \\ -45.0 \\ -122.5 \\ 60.0 \\ 52.5 \\ -115.0 \\ -97.5 \\ 100.0 \end{pmatrix} \Rightarrow \hat{Y} = X_{ij}\alpha_j = \begin{pmatrix} 30 \\ 30 \\ 150 \\ 790 \\ 150 \\ 90 \\ 280 \\ 60 \end{pmatrix} = Y \quad (3)$$

By taking these effects and computing the estimator vector, one gets the same values of the response, *i.e.* the residues are zero. These values can be graphically represented in terms of relative half-effects (Figure 6):

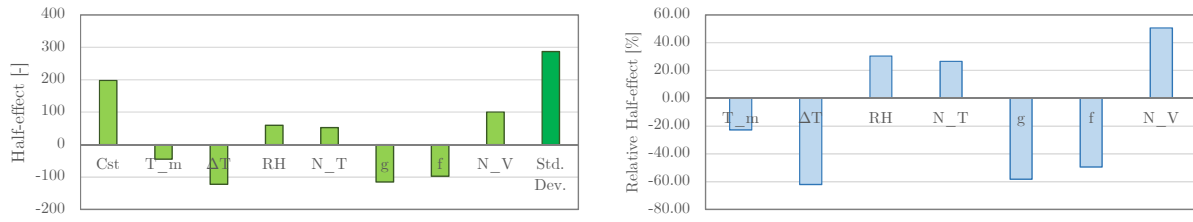


Figure 6: Graphical depiction of the Half Effects with standard error and Relative Half Effects without interactions. “Cst” is the constant, “T_m” the mean temperature, “ΔT” stands for the range, “RH” for dryness, “N_T” the number of thermal cycles, “g” the peak acceleration and “f” the frequency of the vibrations and “N_V” the number of sweeps.

Since there are not enough degrees of freedom left due to the choice of design, an ANOVA table cannot be used as analysis of errors. Hence, a normal plot is made (Figure 7).

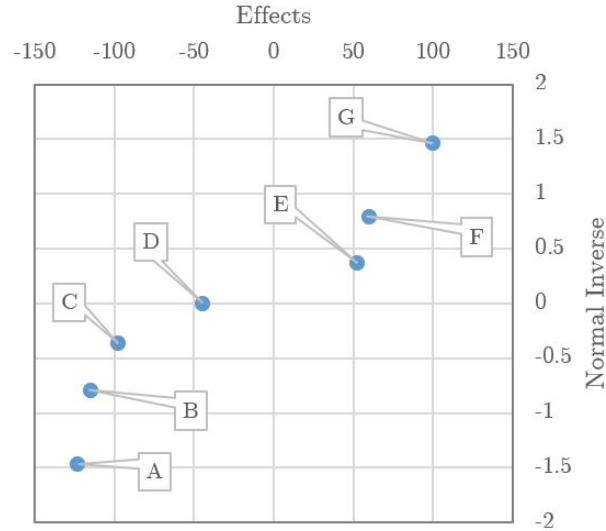


Figure 7: Normal plot of the seven factors half effects.

No particular grouping of the effects occur in the plot, meaning that mostly none of the parameters relates to a random phenomenon. The model – a first degree linear without interaction, would therefore look simply like:

$$\hat{Y} = a_0 + a_1x_1 + a_2x_2 + a_3x_3 + a_4x_4 + a_5x_5 + a_6x_6 + a_7x_7 \quad (4)$$

Linear model with interactions

Let be an extension of the reasoning by considering the 2-by-2 interactions in this 7-factors model:

$$\hat{Y}_{2x2} = \alpha_0 + \sum_{i=1}^7 \alpha_i x_i + \sum_{i<j}^7 \alpha_{ij} x_i x_j + \epsilon_{2x2} \quad (5)$$

The second part of the equation only takes into account until the second order. The matrix of test is then built by multiplying the columns of the core matrix and the resulting model matrix is named X_{2x2} :

| | 1 | 1 | 2 | 3 | 4 | 5 | 6 | 7 | 12 | 13 | 14 | 15 | 16 | 17 | 23 | 24 | 25 | 26 | 27 | 34 | 35 | 36 | 37 | 45 | 46 | 47 | 56 | 57 | 67 | Y | |
|---------|-----|-----|------|----|-----|------|-----|-----|-----|------|------|----|-----|-----|-----|-----|-----|-----|------|-----|-----|------|-----|-----|------|----|-----|------|-----|-----|----|
| Run 1 | 1 | 1 | 1 | 1 | 1 | 1 | 1 | 1 | 1 | 1 | 1 | 1 | 1 | 1 | 1 | 1 | 1 | 1 | 1 | 1 | 1 | 1 | 1 | 1 | 1 | 1 | 1 | 1 | 1 | 30 | |
| Run 2 | 1 | -1 | 1 | -1 | 1 | -1 | 1 | -1 | 1 | -1 | 1 | -1 | 1 | -1 | 1 | -1 | 1 | -1 | 1 | -1 | 1 | -1 | 1 | -1 | 1 | -1 | 1 | -1 | 1 | -1 | 30 |
| Run 3 | 1 | 1 | -1 | -1 | 1 | 1 | -1 | -1 | -1 | -1 | 1 | 1 | -1 | -1 | 1 | -1 | -1 | 1 | 1 | -1 | -1 | 1 | 1 | 1 | -1 | -1 | -1 | -1 | 1 | 150 | |
| Run 4 | 1 | -1 | -1 | 1 | 1 | -1 | -1 | 1 | 1 | -1 | -1 | 1 | 1 | -1 | -1 | -1 | 1 | 1 | -1 | 1 | -1 | -1 | 1 | -1 | -1 | 1 | 1 | -1 | -1 | 790 | |
| Run 5 | 1 | 1 | 1 | 1 | -1 | -1 | -1 | -1 | 1 | 1 | -1 | -1 | -1 | -1 | 1 | -1 | -1 | -1 | -1 | -1 | -1 | -1 | -1 | 1 | 1 | 1 | 1 | 1 | 1 | 150 | |
| Run 6 | 1 | -1 | 1 | -1 | -1 | 1 | -1 | 1 | -1 | 1 | 1 | -1 | 1 | -1 | -1 | -1 | 1 | -1 | 1 | -1 | 1 | -1 | 1 | -1 | -1 | 1 | -1 | -1 | 1 | -1 | 90 |
| Run 7 | 1 | 1 | -1 | -1 | -1 | -1 | 1 | 1 | -1 | -1 | -1 | -1 | 1 | 1 | 1 | 1 | 1 | -1 | -1 | 1 | 1 | -1 | -1 | 1 | -1 | -1 | -1 | -1 | 1 | 280 | |
| Run 8 | 1 | -1 | -1 | 1 | -1 | 1 | 1 | -1 | 1 | -1 | 1 | -1 | -1 | 1 | -1 | -1 | 1 | -1 | 1 | -1 | 1 | 1 | -1 | -1 | 1 | 1 | 1 | -1 | -1 | 60 | |
| HE | 198 | -45 | -123 | 60 | 53 | -115 | -98 | 100 | 60 | -123 | -115 | 53 | 100 | -98 | -45 | -98 | 100 | 53 | -115 | 100 | -98 | -115 | 53 | -45 | -123 | 60 | 60 | -123 | -45 | | |
| RHE [%] | -23 | -62 | 30 | 27 | -58 | -49 | 51 | 30 | -62 | -58 | 27 | 51 | -49 | -23 | -49 | 51 | 27 | -58 | 51 | -49 | -58 | 27 | -23 | -62 | 30 | 30 | -62 | -23 | | | |

1 = Mean temperature, 2 = Temperature range, 3 = Dryness, 4 = Thermal cycles, 5 = Peak acceleration, 6 = Max. frequency, 7 = Vibrations sweeps

Figure 8: Matrix of the model X_{2x2} with interactions, half effects (HE) and relative half effects (RHE).

Using the least square fit algorithm, one finds the values for the half effects and relative half effect, as highlighted in the two bottom lines of the table shown in Figure 8. The normal plot of the comprehensive 2x2 interactions model has been built but provided no valuable information. In order to emphasize any “hidden” interactions, the matrix of aliases (Figure 9) for these effects is computed using the equation below:

$$A = \frac{1}{N} X^T X_{interactions} \quad (6)$$

With X being the model matrix without interaction and $X_{interactions}$ the extended part of the global matrix with interactions (X_{2x2}). Equation 6 results in the matrix shown in Figure 9.

| <i>Fact.</i> | <i>Code</i> | 12 | 13 | 14 | 15 | 16 | 17 | 23 | 24 | 25 | 26 | 27 | 34 | 35 | 36 | 37 | 45 | 46 | 47 | 56 | 57 | 67 |
|--------------|-------------|----|----|----|----|----|----|----|----|----|----|----|----|----|----|----|----|----|----|----|----|----|
| <i>Cst</i> | 0 | 0 | 0 | 0 | 0 | 0 | 0 | 0 | 0 | 0 | 0 | 0 | 0 | 0 | 0 | 0 | 0 | 0 | 0 | 0 | 0 | 0 |
| <i>T_m</i> | 1 | 0 | 0 | 0 | 0 | 0 | 0 | 1 | 0 | 0 | 0 | 0 | 0 | 0 | 0 | 0 | 1 | 0 | 0 | 0 | 0 | 1 |
| ΔT | 2 | 0 | 1 | 0 | 0 | 0 | 0 | 0 | 0 | 0 | 0 | 0 | 0 | 0 | 0 | 0 | 0 | 1 | 0 | 0 | 1 | 0 |
| <i>RH</i> | 3 | 1 | 0 | 0 | 0 | 0 | 0 | 0 | 0 | 0 | 0 | 0 | 0 | 0 | 0 | 0 | 0 | 0 | 1 | 1 | 0 | 0 |
| <i>N_T</i> | 4 | 0 | 0 | 0 | 1 | 0 | 0 | 0 | 0 | 0 | 1 | 0 | 0 | 0 | 0 | 1 | 0 | 0 | 0 | 0 | 0 | 0 |
| <i>g</i> | 5 | 0 | 0 | 1 | 0 | 0 | 0 | 0 | 0 | 0 | 0 | 1 | 0 | 0 | 1 | 0 | 0 | 0 | 0 | 0 | 0 | 0 |
| <i>f</i> | 6 | 0 | 0 | 0 | 0 | 0 | 1 | 0 | 1 | 0 | 0 | 0 | 0 | 1 | 0 | 0 | 0 | 0 | 0 | 0 | 0 | 0 |
| <i>N_V</i> | 7 | 0 | 0 | 0 | 0 | 1 | 0 | 0 | 0 | 1 | 0 | 0 | 1 | 0 | 0 | 0 | 0 | 0 | 0 | 0 | 0 | 0 |

Figure 9: Matrix of aliases A and highlighting of the non-zero values.

The corresponding table of contrasts is then built by combining the non-zero values of A (Equation 7).

$$\begin{cases}
 l_0 = a_0 \\
 l_1 = a_1 + a_{23} + a_{45} + a_{67} & (1 = \text{Mean temperature}) \\
 l_2 = a_2 + a_{13} + a_{46} + a_{57} & (2 = \text{Temperature range}) \\
 l_3 = a_3 + a_{12} + a_{47} + a_{56} & (3 = \text{Dryness}) \\
 l_4 = a_4 + a_{15} + a_{26} + a_{37} & (4 = \text{Thermal cycles}) \\
 l_5 = a_5 + a_{14} + a_{27} + a_{36} & (5 = \text{Peak acceleration}) \\
 l_6 = a_6 + a_{17} + a_{24} + a_{35} & (6 = \text{Max. frequency}) \\
 l_7 = a_7 + a_{16} + a_{25} + a_{34} & (7 = \text{Vibration sweeps})
 \end{cases} \quad (7)$$

One can see from Equation 7 that the interactions effects are aliased with the main effects. Expected interactions are:

- It is likely that a given thermal factor (a_{1-4}) shows interactions with the other thermal factors. Therefore are relevant the thermal cross-factors: a_{12} , a_{13} , a_{14} , a_{23} , a_{24} , a_{34} .
- It is likely that a given mechanical factor (a_{5-7}) shows interactions with the other mechanical factors, hence for the mechanical counterpart: a_{56} , a_{57} , a_{67} .
- The relation between the thermal and the mechanical parameters is not obvious. Imagining that it may depend on combined effect of a thermomechanical fatigue-related phenomenon, it would concern the rest of the 2x2 coefficients that appear in Equation 7.
- It could be possible that the contrasts l_{1-4} only comprise the thermal 2x2 cross-factors, while l_{5-7} only are aliased by the mechanical 2x2 cross-factors.

Since the interactions effects are pure alias, a Pareto chart can also be used to represent the main effects' importance. By considering only the magnitude (absolute value) of the half effects (since a Pareto chart by definition can only have positive values), one gets (Figure 10).

The values obtained for the half effects in Figure 8 permit to compute the estimated response for the number of shocks following a model with interactions (Equation 8).

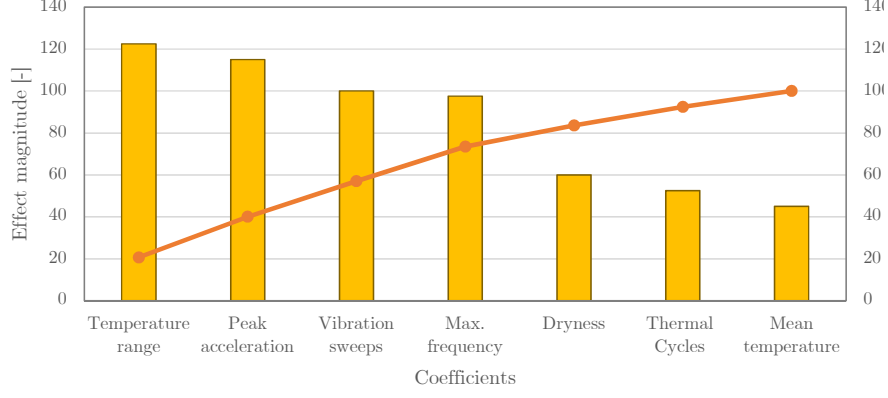


Figure 10: Pareto chart of the main effects of the model with interactions.

$$Y_i - \hat{Y}_i = \epsilon_{2 \times 2} = \begin{pmatrix} 502.5 \\ 502.5 \\ 142.5 \\ -1778 \\ 142.5 \\ 322.5 \\ -247.5 \\ 412.5 \end{pmatrix} \quad (8)$$

These residues are greater than the response, which indicates that the full model with interactions is not an relevant way to model the experiment. As an extension to the experiment, de-aliasing of the effects would be imaginable and alleviate the doubts, provided 8 more samples through mean of a full-foldover design. This method would enable to separate the main effects from the interactions.

Discussion and conclusion

On the thermal/humidity side, the plot of relative half effects (Figure 5) shows that the range of cycling has a more detrimental effect on the device's lifetime compared to the mean temperature. This is an interesting finding, since that could imply that failure could be more likely linked to thermal fatigue phenomena, rather than a purely Arrhenius-based accelerated aging. Humidity (through "Dryness") is the second most important factor in this part, which shows a positive impact on the lifetime (as expected for MEMS): lower is the humidity, longer is the live of the device. Dryness, Mean temperature and Range of cycling are most likely correlated. Interestingly, the number of cycles – within the frame of this experiment – does not appear as a predominant factor. Surprisingly, the greater the number of cycles, the greater the lifetime. This outcome is consistent with the fact that a polymeric packaging filled with a damping gel should degrade faster compared to the ceramic/metallic counterparts. Has to be noted that a full scale reliability study (50 cycles) would maybe bring to a different result. Finally, the normal plot indicated that, most likely, none of these factors is random.

On the mechanical side, the global view shows that all of the three factors (peak acceleration, maximum frequency and vibration sweeps) have big impact on the lifetime. The acceleration peak of vibration is

slightly more detrimental than the maximum frequency. On the other side, the increasing number of cycles seems here to also increase the lifetime of the device. A second run of experiments would maybe contradict this statement.

Despite the normal plot indicating that most of the points are not normal, the model with interactions cannot represent correctly the experiment, as shown by the large values of the residues. Nevertheless, a better knowledge of the outcome of a multi-parameter reliability assessment has been obtained. It would now be interesting, as future development, to extend the test plan with a focus on the most severe effects, increase the number of cycles and possibly apply the fractional factorial design.

References

- [1] Swiss Center for Electronics and Microtechnology (CSEM), *Technical Memorandum: Test programme for reliability assessment of MEMS products*, 2016.
- [2] J.-M. Fuerbringer, *Design of Experiments (Doctoral Program in Robotics, Control and Intelligent Systems)*, 2016.
- [3] NIST/SEMATECH e-Handbook of Statistical Methods, <http://www.itl.nist.gov/div898/handbook/>, consulted in January 2018.